

Infrared Spectroscopic and Density Functional Theory Study on the Reactions of Lanthanum Atoms with Carbon Dioxide in Rare-Gas Matrices

Ling Jiang and Qiang Xu*

National Institute of Advanced Industrial Science and Technology (AIST), Ikeda, Osaka 563-8577, Japan, and Graduate School of Science and Technology, Kobe University, Nada Ku, Kobe, Hyogo 657-8501, Japan

Received: February 13, 2007; In Final Form: March 12, 2007

Reactions of laser-ablated La atoms with CO₂ molecules in solid argon and neon have been investigated using matrix-isolation infrared spectroscopy. On the basis of isotopic shifts, mixed isotopic splitting patterns, and CCl₄-doping experiments, absorptions at 1839.9 and 753.6 cm⁻¹ in argon and 1855.9 and 771.3 cm⁻¹ in neon are assigned to the C–O and La–O stretching vibrations of the OLaCO molecule, respectively. Ultraviolet–visible photoinduced isomerization of OLaCO to La-(η^2 -OC)O and OLa-(η^2 -CO) have been observed under different wavelength photolyses in the solid matrix. The neon matrix experiments give the C–O and La–O stretching vibrations of the OLaCO⁻ anion at 1769.5 and 779.3 cm⁻¹, respectively. Density functional theory calculations have been performed on these products, which support the experimental assignments of the infrared spectra. The present study reveals that the C–O stretching vibrational frequencies of OMCO decrease from Sc to La, which indicates an increase in metal d orbital \rightarrow CO π^* back-donation in this series.

Introduction

The interaction of metal atoms with small molecules (i.e., CO, O₂, CO₂, H₂, etc.) is of considerable interest because of its importance in a great number of catalytic processes.¹ Among these small molecules, metal-catalyzed activation of carbon dioxide has become an important subject of research in organometallic and catalytic surface chemistry for many years.^{2–6} Extensive efforts have been made to recycle CO₂ from industrial emission and to remove some of this greenhouse gas.^{2–8} Reactions of various metal atoms with carbon dioxide have been investigated and a series of metal carbon dioxide complexes have been experimentally characterized.^{9–29} Quantum chemical calculations have been performed to understand the electronic structures and bonding characteristics of these complexes.^{9–32} Insertion to produce OMCO has been observed for all the first-row transition metal atoms except Cu and Zn in the rare-gas matrices.^{13–21} The reactions of Cr through Cu atoms with CO₂ give the OMCO⁻ anions and Co, Ni, and Cu atoms also produce the addition MCO₂⁻ anions.^{13–21}

Recent studies have shown that, with an aid of isotopic substitution technique, matrix isolation infrared spectroscopy combined with quantum chemical calculation is very powerful in investigating the spectrum, structure, and bonding of novel species.^{33,34} In contrast with extensive experimental and theoretical studies of the interactions of CO₂ molecules with the transition-metal and main-group-element atoms,^{9–29} however, much less work has been done on the La + CO₂ reactions. Recently, argon matrix investigations of the reactions of laser-ablated group 3 metal atoms with the valence isoelectronic CS₂ and OCS molecules have characterized the SMCX and S–M(η^2 -CX) (X = S or O) molecules.³⁵ Gas-phase reactions of atomic lanthanide cations with CO₂ and CS₂ reveal a periodicity in reaction efficiency for the kinetics of O-atom

transfer from CO₂, whereas unit efficiency is observed for S-atom transfer from CS₂.³⁶ Here we report a study of reactions of laser-ablated lanthanum atoms with carbon dioxide in solid argon and neon. We will show that the insertion OLaCO molecule is formed during sample deposition and slightly increased on annealing. Ultraviolet–visible photoinduced rearrangements of OLaCO to La-(η^2 -OC)O and OLa-(η^2 -CO) are observed under different wavelength photolyses. IR spectroscopy also provides evidence for the formation of the OLaCO⁻ molecule.

Experimental and Theoretical Methods

The experiment for laser ablation and matrix isolation infrared spectroscopy is similar to those previously reported.^{37,38} In short, the Nd:YAG laser fundamental (1064 nm, 10 Hz repetition rate with 10 ns pulse width) was focused on the rotating La target. The laser-ablated La atoms were co-deposited with CO₂ in excess argon (or neon) onto a CsI window cooled normally to 4 K by means of a closed-cycle helium refrigerator. Typically, 1–12 mJ/pulse laser power was used. CO₂ (99.99%, Takachiho Chemical Industrial Co., Ltd), ¹³C¹⁶O₂ (99%, ¹⁸O < 1%, Cambridge Isotopic Laboratories), ¹²C¹⁸O₂ (95%, Cambridge Isotopic Laboratories), ¹²C¹⁶O₂ + ¹³C¹⁶O₂, and ¹²C¹⁶O₂ + ¹²C¹⁸O₂ were used in different experiments. In general, matrix samples were deposited for 30–60 min with a typical rate of 2–4 mmol/h. After sample deposition, IR spectra were recorded on a BIO-RAD FTS-6000e spectrometer at 0.5 cm⁻¹ resolution using a liquid nitrogen cooled HgCdTe (MCT) detector for the spectral range of 5000–400 cm⁻¹. Samples were annealed at different temperatures and subjected to different wavelength photolyses for 10–15 min using a high-pressure mercury arc lamp (Ushio, 100 W, λ > 250 nm) with and without a UV cutoff filter (λ > 480 nm).

Density functional theory (DFT) calculations were performed to predict the structures and vibrational frequencies of the observed reaction products using the Gaussian 03 program.³⁹

* Author to whom correspondence should be addressed. E-mail: q.xu@aist.go.jp.

TABLE 1: IR Absorptions (in cm^{-1}) Observed from Co-Deposition of Laser-Ablated La Atoms with CO_2 in Excess Argon and Neon at 4 K

	$^{12}\text{C}^{16}\text{O}_2$	$^{13}\text{C}^{16}\text{O}_2$	$^{12}\text{C}^{18}\text{O}_2$	$R(12/13)$	$R(16/18)$	assignment	
Ar	1843.2	1802.0	1800.5	1.0229	1.0237	OLaCO site	
	1839.9	1798.8	1797.4	1.0228	1.0236	OLaCO	
	1644.8	1602.0	1600.0	1.0267	1.0280	OLa-(η^2 -CO)	
	1626.9	1591.3	1593.4	1.0224	1.0210	La-(η^2 -OC)O	
	827.0	827.0	784.6	1.0000	1.0540	OLa-(η^2 -CO)	
	796.8	796.8	756.2	1.0000	1.0537	LaO	
	762.1	762.1	723.0	1.0000	1.0541	(O_2)LaO	
	753.6	753.6	714.9	1.0000	1.0541	OLaCO	
	Ne	1855.9	1814.5	1812.7	1.0228	1.0238	OLaCO
		1769.5	1726.0	1734.9	1.0252	1.0199	OLaCO ⁻
808.7		808.7	767.5	1.0000	1.0537	LaO	
779.3		779.3	739.4	1.0000	1.0540	OLaCO ⁻	
771.3		771.3	732.0	1.0000	1.0537	OLaCO	

The BPW91 and B3LYP density functional methods were used.⁴⁰ The 6-311+G(d) basis set was used for the C and O atoms,⁴¹ and the Stevens/Basch/Krauss ECP split valence (CEP-31G) for the La atom.⁴² Geometries were fully optimized and vibrational frequencies were calculated with analytical second derivatives. The previous investigations have shown that DFT calculations can provide reliable information for metal complexes, such as infrared frequencies, relative absorption intensities, and isotopic shifts.^{9–38}

Results and Discussion

Experiments have been done with carbon dioxide concentrations ranging from 0.02% to 2.0% in excess argon and neon. Typical infrared spectra for the reactions of laser-ablated La atoms with CO_2 molecules in excess argon and neon in the selected regions are illustrated in Figures 1–4, and the absorption bands in different isotopic experiments are listed in Table 1. The stepwise annealing and photolysis behavior of the product absorptions is also shown in the figures and will be discussed below. Experiments were also done with different concentrations of CCl_4 serving as an electron scavenger.

Quantum chemical calculations have been carried out for the possible isomers and electronic states of the potential product molecules. Figure 5 shows the optimized structures of the possible reaction products. The comparison of the observed and calculated isotopic frequency ratios for the C–O and La–O stretching modes of the products are summarized in Table 2. The ground electronic states, point groups, vibrational frequencies, and intensities are listed in Table 3.

OLaCO. In the reaction of La atoms with CO_2 in the argon matrix, two sharp absorptions at 1839.9 and 753.6 cm^{-1} are present together during sample deposition, slightly increased after sample annealing to 25 K, markedly decreased upon $\lambda > 480$ nm irradiation, and little changed after further annealing to higher temperature (Table 1 and Figure 1). The 1839.9 cm^{-1} band shifts to 1798.8 cm^{-1} with $^{13}\text{C}^{16}\text{O}_2$ and to 1797.4 cm^{-1} with $^{12}\text{C}^{18}\text{O}_2$, exhibiting isotopic frequency ratios ($^{12}\text{C}^{16}\text{O}_2/^{13}\text{C}^{16}\text{O}_2$, 1.0228; $^{12}\text{C}^{16}\text{O}_2/^{12}\text{C}^{18}\text{O}_2$, 1.0236) characteristic of C–O stretching vibrations. The mixed $^{12}\text{C}^{16}\text{O}_2 + ^{13}\text{C}^{16}\text{O}_2$ and $^{12}\text{C}^{16}\text{O}_2 + ^{12}\text{C}^{18}\text{O}_2$ isotopic spectra (Figure 2) only provide the sum of pure isotopic bands, which indicates only one CO unit is involved in this carbonyl stretching mode.⁴³ The 753.6 cm^{-1} band shows no carbon isotopic shift, but shifts to 714.9 cm^{-1} with $^{12}\text{C}^{18}\text{O}_2$. The $^{12}\text{C}^{16}\text{O}_2/^{12}\text{C}^{18}\text{O}_2$ isotopic frequency ratio of 1.0541 is very close to the diatomic $\text{La}^{16}\text{O}/\text{La}^{18}\text{O}$ frequency ratio of 1.0537,⁴⁴ suggesting a La–O stretching mode. Only doublets have been observed in the $^{12}\text{C}^{16}\text{O}_2 + ^{12}\text{C}^{18}\text{O}_2$ isotopic spectra (Figure 2). Furthermore, doping with CCl_4 has no effect

on these bands (not shown here), suggesting that the product is neutral.⁴⁵ The 1839.9 and 753.6 cm^{-1} bands are therefore assigned to the C–O and La–O stretching vibrations of the neutral OLaCO. The corresponding C–O and La–O stretching frequencies of OLaCO in solid neon appear at 1855.9 and 771.3 cm^{-1} (Table 1 and Figures 3 and 4), respectively, which are 16.0 and 17.7 cm^{-1} blue-shifted from the argon matrix counterpart. The absorptions of the analogous OScCO and OYCO molecules have been observed at 1873.4, 894.1, 1861.5, and 796.5 cm^{-1} in the previous argon matrix experiments, respectively.¹³

Both BPW91 and B3LYP calculations predict that the OLaCO molecule has a C_s symmetry with an $^2A''$ ground state (Table 3 and Figure 5), which lies ca. 63 kcal/mol lower in energy than a $^4A'$ one. For the C–O stretching mode, the vibrational frequency is calculated to be 1907.7 cm^{-1} with the $^{12}\text{C}^{16}\text{O}_2/^{13}\text{C}^{16}\text{O}_2$ and $^{12}\text{C}^{16}\text{O}_2/^{12}\text{C}^{18}\text{O}_2$ isotopic frequency ratios of 1.0231 and 1.0243 at the BPW91/6-311+G(d)-CEP-31G level (Tables 2 and 3), respectively, which are consistent with the experimental observations. The La–O stretching vibration is predicted to be 720.2 cm^{-1} , and the calculated $^{12}\text{C}^{16}\text{O}_2/^{12}\text{C}^{18}\text{O}_2$ isotopic frequency ratio of 1.0540 is in accord with the experimental value of 1.0541 (Table 2). The agreements between the experimental and calculated results have also been obtained at the B3LYP/6-311+G(d)-CEP-31G level (Table 2). Recent studies indicate that in most cases, the BPW91 functional gives calculated $\nu_{\text{C-O}}$ and $\nu_{\text{M-O}}$ frequencies much closer to the experimental values than the B3LYP functional.^{29,45} Hereafter, mainly BPW91 results are presented for discussions.

La-(η^2 -OC)O. The absorption at 1626.9 cm^{-1} with La and CO_2 in solid argon appears upon $\lambda > 480$ nm irradiation, disappears after broad-band irradiation, and does not recover after further annealing (Table 1 and Figure 1). This band shifts to 1591.3 cm^{-1} with $^{13}\text{C}^{16}\text{O}_2$ and to 1593.4 cm^{-1} with $^{12}\text{C}^{18}\text{O}_2$, giving $^{12}\text{C}^{16}\text{O}_2/^{13}\text{C}^{16}\text{O}_2$ and $^{12}\text{C}^{16}\text{O}_2/^{12}\text{C}^{18}\text{O}_2$ isotopic frequency ratios of 1.0224 and 1.0210, which exhibits a larger carbon-13 shift than oxygen-18 shift. The mixed $^{12}\text{C}^{16}\text{O}_2 + ^{13}\text{C}^{16}\text{O}_2$ and $^{12}\text{C}^{16}\text{O}_2 + ^{12}\text{C}^{18}\text{O}_2$ isotopic spectra (Figure 2) only provide the sum of pure isotopic bands. Note that the 1626.9 cm^{-1} band appears after $\lambda > 480$ nm irradiation while the absorptions of the OLaCO molecule sharply decrease, indicating that this new product is the isomer of the OLaCO molecule. By analogy with the M-(η^2 -OC)O (M = Sc, Y) spectra,¹³ the 1626.9 cm^{-1} band is assigned to the antisymmetric O–C–O stretching mode of La-(η^2 -OC)O. The corresponding IR absorptions of the La-(η^2 -OC)O molecule in solid neon are absent from the present matrix spectra.

DFT calculations have been performed for the La-(η^2 -OC)O molecule, and these support the above assignments. The La-(η^2 -OC)O molecule is predicted to have a C_s symmetry with an $^2A''$ ground state (Table 3 and Figure 5), which lies 11 kcal/mol higher in energy than the OLaCO isomer. The antisymmetric O–C–O stretching vibrational frequency is calculated at 1701.2 cm^{-1} (700 km/mol) with the $^{12}\text{C}^{16}\text{O}_2/^{13}\text{C}^{16}\text{O}_2$ and $^{12}\text{C}^{16}\text{O}_2/^{12}\text{C}^{18}\text{O}_2$ isotopic frequency ratios of 1.0241 and 1.0226 (Tables 2 and 3), respectively, which are consistent with the experimental observations. The symmetric O–C–O stretching and La–O stretching vibrations are predicted to be 866.5 and 696.5 cm^{-1} , respectively, which have relatively small intensities (106 and 68 km/mol) and are not readily to be observed, consistent with the absence from the present experiments.

OLa-(η^2 -CO). In the reaction of La atoms with CO_2 in the argon matrix, two sharp absorptions at 1644.8 and 827.0 cm^{-1} are produced together after broad-band irradiation, and slightly

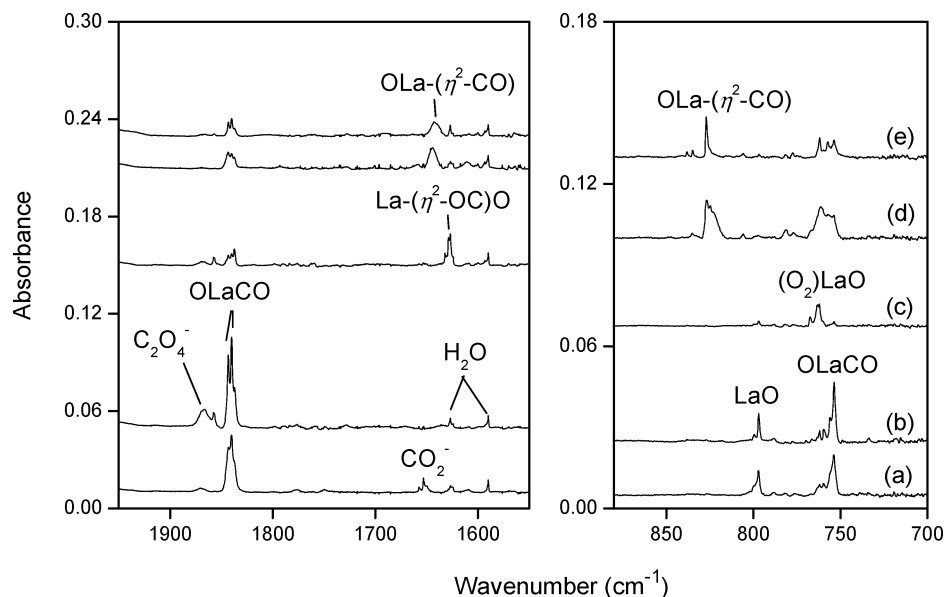


Figure 1. Infrared spectra in the 1950–1550 and 850–700 cm^{-1} regions from co-deposition of laser-ablated La atoms with 0.8% CO_2 in Ar. (a) 1 h of sample deposition at 4 K, (b) after annealing to 25 K, (c) after 12 min of $\lambda > 480$ nm irradiation, (d) after 10 min of broad-band irradiation, and (e) after annealing to 30 K.

TABLE 2: Comparison of Observed and Calculated IR Frequency Ratios for the Products

species	vibrational mode	experimental		method	calculated	
		$R(12/13)$	$R(16/18)$		$R(12/13)$	$R(16/18)$
OLaCO (in Ar)	$\nu_{\text{C-O}}$	1.0228	1.0236	BPW91	1.0231	1.0243
	$\nu_{\text{La-O}}$	1.0000	1.0541	B3LYP	1.0230	1.0244
La-(η^2 -OC)O (in Ar)	$\nu_{\text{C-O}}$	1.0224	1.0210	BPW91	1.0000	1.0540
	$\nu_{\text{La-O}}$	1.0000	1.0540	B3LYP	1.0241	1.0226
OLa-(η^2 -CO) (in Ar)	$\nu_{\text{C-O}}$	1.0267	1.0280	BPW91	1.0228	1.0248
	$\nu_{\text{La-O}}$	1.0000	1.0540	B3LYP	1.0228	1.0247
OLaCO ⁻ (in Ne)	$\nu_{\text{C-O}}$	1.0252	1.0199	BPW91	1.0000	1.0540
	$\nu_{\text{La-O}}$	1.0000	1.0540	B3LYP	1.0000	1.0541

TABLE 3: Ground Electronic States, Point Groups, Vibrational Frequencies (cm^{-1}) and Intensities (km/mol) of the Reaction Products Calculated at the BPW91/6-311+G(d)-CEP-31G Level

species	elec state	point group	frequency (intensity, mode)
OLaCO	$^2A''$	C_s	1907.7 (1008, A), 720.2 (150, A), 278.9 (3, A), 237.7 (1, A), 217.9 (17, A), 53.5 (17, A)
La-(η^2 -OC)O	$^2A''$	C_s	1701.2 (700, A), 866.5 (106, A), 696.5 (68, A), 367.7 (7, A), 332.7 (0.1, A), 253.0 (11, A)
OLa-(η^2 -CO)	2A	C_1	1704.5 (663, A), 727.8 (156, A), 259.2 (6, A), 222.9 (4, A), 147.6 (4, A), 91.7 (19, A)
OLaCO ⁻	$^3A''$	C_s	1826.3 (837, A), 678.3 (199, A), 260.8 (10, A), 220.5 (1, A), 208.1 (2, A), 93.8 (4, A)

decrease after further annealing to 30 K (Table 1 and Figure 1). The 1644.8 cm^{-1} band shifts to 1602.0 cm^{-1} with $^{13}\text{C}^{16}\text{O}_2$ and to 1600.0 cm^{-1} with $^{12}\text{C}^{18}\text{O}_2$, exhibiting isotopic frequency ratios ($^{12}\text{C}^{16}\text{O}_2/^{13}\text{C}^{16}\text{O}_2$, 1.0267; $^{12}\text{C}^{16}\text{O}_2/^{12}\text{C}^{18}\text{O}_2$, 1.0280) characteristic of C–O stretching vibrations. The mixed $^{12}\text{C}^{16}\text{O}_2 + ^{13}\text{C}^{16}\text{O}_2$ and $^{12}\text{C}^{16}\text{O}_2 + ^{12}\text{C}^{18}\text{O}_2$ isotopic spectra (Figure 2) only provide the sum of pure isotopic bands, indicating that only one CO unit is involved in this carbonyl stretching mode.⁴³ The very low C–O stretching vibrational frequency of 1644.8 cm^{-1} is reminiscent of the side-on-bonded structure of the OSc-(η^2 -CO) and OY-(η^2 -CO) molecules, in which the corresponding frequencies have been observed at 1613.9 and 1614.5 cm^{-1} in the previous argon matrix experiments, respectively.¹³ On the other hand, the associated 827.0 cm^{-1} band shows no carbon isotopic shift, but shifts to 784.6 cm^{-1} with $^{12}\text{C}^{18}\text{O}_2$, suggesting a terminal La–O stretching vibration. Only doublets

have been observed in the mixed isotopic spectra, indicating that only one O atom is involved in this mode.⁴³ The 1644.8 and 827.0 cm^{-1} bands appear together after broad-band irradiation at the expense of the La-(η^2 -OC)O molecule, indicating that this new product also has the LaCO₂ stoichiometry. The 1644.8 and 827.0 cm^{-1} bands are therefore assigned to the C–O and La–O stretching vibrations of the OLa-(η^2 -CO) molecule. The corresponding IR absorptions of OLa-(η^2 -CO) in solid neon are absent from the present matrix experiments.

Our BPW91 calculations predict the OLa-(η^2 -CO) molecule to have a C_1 symmetry with a 2A ground state (Table 3 and Figure 5), which lies 8 kcal/mol higher in energy than the OLaCO isomer. The C–O and La–O stretching vibrational frequencies are calculated at 1704.5 and 727.8 cm^{-1} . The C–O bond length in the OLa-(η^2 -CO) molecule is predicted to be

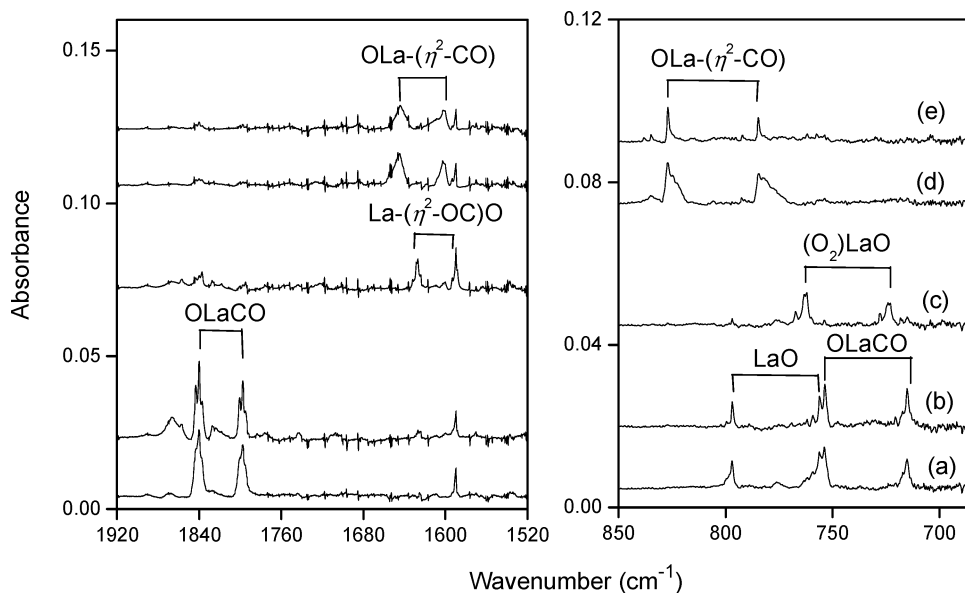


Figure 2. Infrared spectra in the 1950–1550 and 850–700 cm^{-1} regions for laser-ablated La atoms co-deposited with 0.6% $^{12}\text{C}^{16}\text{O}_2$ + 0.6% $^{12}\text{C}^{18}\text{O}_2$ in Ar. (a) 1 h of sample deposition at 4 K, (b) after annealing to 25 K, (c) after 12 min of $\lambda > 480$ nm irradiation, (d) after 10 min of broad-band irradiation, and (e) after annealing to 30 K.

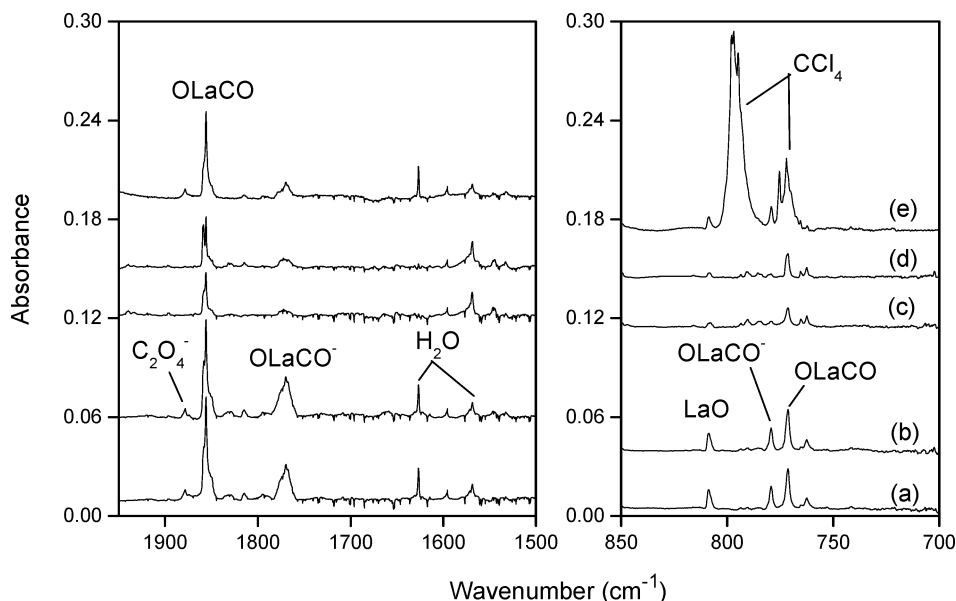


Figure 3. Infrared spectra in the 1950–1550 and 850–700 cm^{-1} regions from co-deposition of laser-ablated La atoms with 0.3% CO_2 in Ne. (a) 30 min of sample deposition at 4 K, (b) after annealing to 8 K, (c) after 10 min of broad-band irradiation, (d) after annealing to 10 K, and (e) 0.3% CO_2 + 0.04% CCl_4 , after annealing to 8 K.

1.197 Å, which is 0.029 Å longer than that in the OLaCO molecule but 0.171 Å shorter than that in the $\text{La}(\eta^2\text{-OC})\text{O}$ molecule.

OLaCO⁻. In the reaction of La atoms with CO_2 in the neon matrix, the absorptions at 1769.5 and 779.3 cm^{-1} appear together during sample deposition, change little after annealing to 8 K, sharply decrease after photolysis, and do not return after further annealing to higher temperature (Table 1 and Figure 3). The upper 1769.5 cm^{-1} band shifts to 1726.0 cm^{-1} with $^{13}\text{C}^{16}\text{O}_2$ and to 1734.9 cm^{-1} with $^{12}\text{C}^{18}\text{O}_2$, exhibiting isotopic frequency ratios ($^{12}\text{C}^{16}\text{O}_2/^{13}\text{C}^{16}\text{O}_2$, 1.0252; $^{12}\text{C}^{16}\text{O}_2/^{12}\text{C}^{18}\text{O}_2$, 1.0199) characteristic of C–O stretching vibrations. The mixed $^{12}\text{C}^{16}\text{O}_2$ + $^{13}\text{C}^{16}\text{O}_2$ and $^{12}\text{C}^{16}\text{O}_2$ + $^{12}\text{C}^{18}\text{O}_2$ isotopic spectra (Figure 4) only provide the sum of pure isotopic bands, which indicates only one CO unit is involved in this carbonyl stretching mode.⁴³ The 779.3 cm^{-1} band shows no carbon isotopic shift, but shifts to

739.4 cm^{-1} with $^{12}\text{C}^{18}\text{O}_2$. The $^{12}\text{C}^{16}\text{O}_2/^{12}\text{C}^{18}\text{O}_2$ isotopic frequency ratio of 1.0540 is very close to the diatomic $\text{La}^{16}\text{O}/\text{La}^{18}\text{O}$ frequency ratio of 1.0537,⁴⁴ suggesting a La–O stretching mode. Only doublets have been observed in the $^{12}\text{C}^{16}\text{O}_2$ + $^{12}\text{C}^{18}\text{O}_2$ isotopic spectra (Figure 4). Furthermore, doping with CCl_4 markedly decreases these bands (Figure 3, trace e), suggesting that the product is anionic.⁴⁵ Accordingly, the 1769.5 and 779.3 cm^{-1} bands are assigned to the C–O and La–O stretching vibrations of the OLaCO⁻ anion. The argon counterpart of OLaCO⁻ is absent from the present matrix experiments.

Our DFT calculations predict the OLaCO⁻ molecule to have an $^3\text{A}'$ ground state with C_s symmetry (Table 3 and Figure 5). The calculated C–O and La–O stretching vibrational frequencies are 1826.3 and 678.3 cm^{-1} , respectively. The $\angle\text{LaCO}$ angle

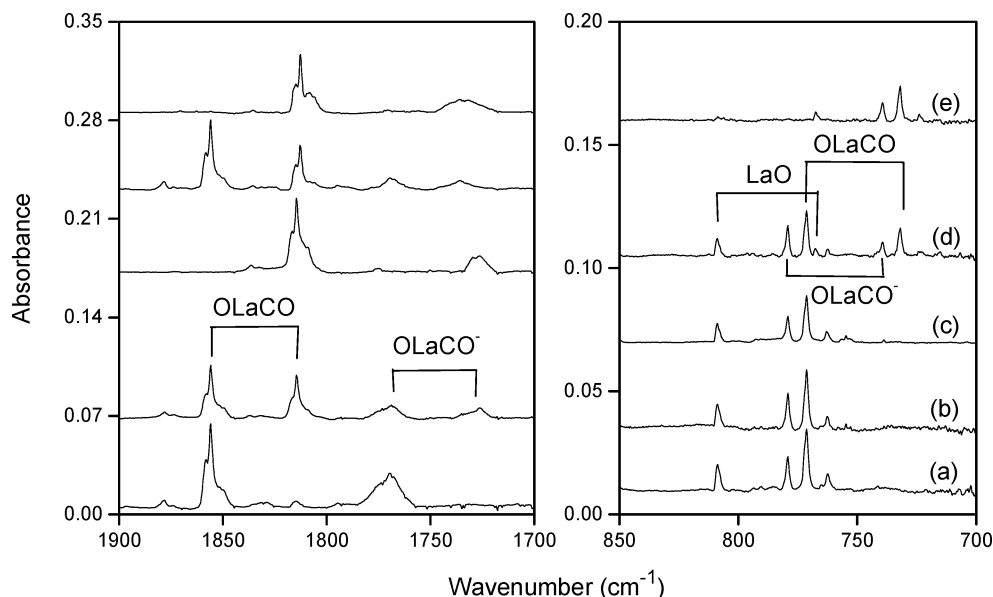


Figure 4. Infrared spectra in the 1900–1700 and 850–700 cm^{-1} regions from co-deposition of laser-ablated La atoms with isotopic CO_2 in Ne after annealing to 8 K. (a) 0.3% $^{12}\text{C}^{16}\text{O}_2$, (b) 0.2% $^{12}\text{C}^{16}\text{O}_2$ + 0.2% $^{13}\text{C}^{16}\text{O}_2$, (c) 0.3% $^{13}\text{C}^{16}\text{O}_2$, (d) 0.2% $^{12}\text{C}^{16}\text{O}_2$ + 0.2% $^{12}\text{C}^{18}\text{O}_2$, and (e) 0.3% $^{12}\text{C}^{18}\text{O}_2$.

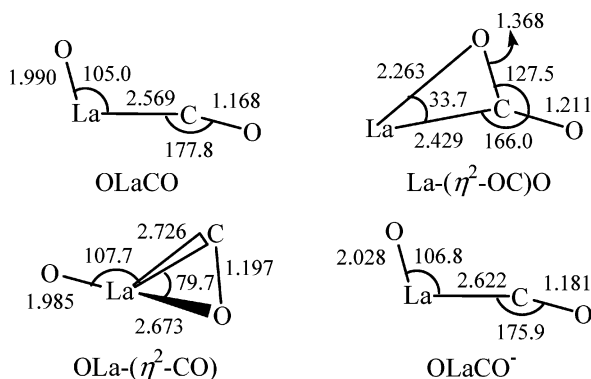


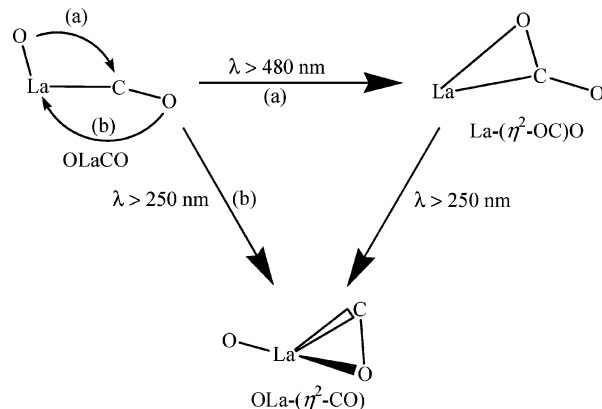
Figure 5. Optimized structures (bond lengths in angstrom, bond angles in degree) of the possible reaction products calculated at the BPW91/6-311+G(d)-CEP-31G level.

in the anionic OLaCO^- molecule (175.9°) is slightly smaller than in the neutral OLaCO molecule (177.8°) (Figure 5).

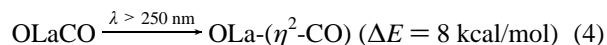
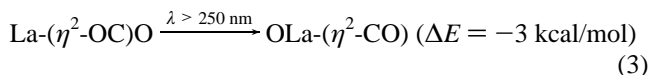
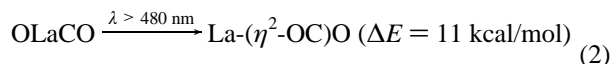
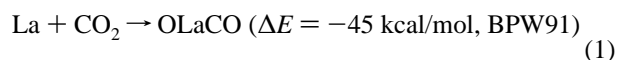
It is noted that the calculated $\nu_{\text{C}-\text{O}}$ frequencies are consistently $65 \pm 8 \text{ cm}^{-1}$ higher and the calculated $\nu_{\text{La}-\text{O}}$ frequencies are consistently 100 cm^{-1} lower than the experimental values (Tables 1 and 3), respectively. Such systematic difference between the calculated C–O and La–O stretching vibrational frequencies with the experimental values of the lanthanide complexes may be due to the inefficiency of the XC functional and/or the basis sets used here.

Reaction Mechanism. At the present experimental conditions, the IR absorptions of the OLaCO molecule appear during sample deposition and slightly increase upon annealing in the reactions of laser-ablated lanthanum atoms with carbon dioxide molecules in the argon and neon matrices (Figure 1), suggesting that this product may be mainly formed during the co-deposition of CO_2 with laser-ablated La atoms (reaction 1). This insertion is predicted to be exothermic by about 45 kcal/mol (BPW91). The $\text{La}-(\eta^2\text{-OC})\text{O}$ molecule is produced after UV irradiation using the 480 nm long-wavelength pass filter while the absorptions of the OLaCO molecule is sharply destroyed (Figure 1), which implies photoisomerization reaction 2. The rearrangement of OLaCO to $\text{La}-(\eta^2\text{-OC})\text{O}$ is calculated to be slightly endothermic by 11 kcal/mol. The absorptions of $\text{OLa}-(\eta^2\text{-CO})$

SCHEME 1

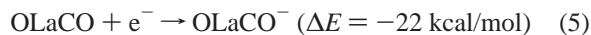


appear after broad-band irradiation at the expense of $\text{La}-(\eta^2\text{-OC})\text{O}$ (Figure 1), indicating photoisomerization reaction 3. It is noted that the $\text{OLa}-(\eta^2\text{-CO})$ molecule can be directly generated after broad-band irradiation at the expense of OLaCO in the present experiments (not shown here), implying photoisomerization reaction 4. The photochemistry is illustrated in Scheme 1. Similar ultraviolet–visible photoinduced isomerizations have also been observed for the Sc and Y systems:¹³



Recent investigations have shown that laser ablation of metal targets produces not only neutral metal atoms, but also metal cations and electrons, and ionic metal complexes can also be formed in the reactions with small molecules.⁴⁵ In the present experiments, the OLaCO^- anion appears during sample deposi-

tion and changes little after sample annealing (Figure 3), suggesting that this anion may be generated by electron capture by neutral OLaCO during co-deposition (reaction 5):



It is interesting to compare the observed C–O stretching vibrational frequencies of OMCO (M = Sc, Y, and La) in the argon matrix. The C–O stretching vibrational frequencies of OMCO decrease from Sc to La (1873.4,¹³ 1861.5,¹³ 1839.9 cm⁻¹), which indicates an increase in metal d orbital → CO π* back-donation in this series. A similar trend holds true for the M–O stretching vibrational frequencies of these OMCO molecules (894.1,¹³ 796.5,¹³ 753.6 cm⁻¹). A similar decreasing trend in metal carbonyl frequencies going down the group 3 metals is also found for the MCO⁺ (M = Sc, Y, and La) cations and the early transition metals carbonyls (groups 4–6),^{46–48} but the reverse trend is found for the late transition metals (groups 8–10).^{47,49–52}

Conclusions

Reactions of laser-ablated lanthanum atoms with carbon dioxide molecules in solid argon and neon have been investigated using matrix-isolation infrared spectroscopy. The insertion product, OLaCO, has been formed during sample deposition and identified on the basis of isotopic shifts, mixed isotopic splitting patterns, and CCl₄-doping experiments. Ultraviolet–visible photoinduced rearrangements of OLaCO to La-(η²-OC)O and OLa-(η²-CO) have been observed under different wavelength photolyses in the argon matrix. IR spectroscopy also provides evidence for the formation of the OLaCO⁻ molecule in the neon matrix. Density functional theory calculations have been performed on these products. The agreement between the experimental and calculated vibrational frequencies, relative absorption intensities, and isotopic shifts supports the identification of these species from the matrix infrared spectra. The present study reveals that the C–O stretching vibrational frequencies of OMCO decrease from Sc to La, which indicates an increase in metal d orbital → CO π* back-donation in this series.

Acknowledgment. We gratefully acknowledge financial support for this research by a Grant-in-Aid for Scientific Research (B) (Grant No. 17350012) from the Ministry of Education, Culture, Sports, Science and Technology (MEXT) of Japan. L.J. thanks MEXT of Japan and Kobe University for Honors Scholarship.

References and Notes

- (1) Cotton, F. A.; Wilkinson, G.; Murillo, C. A.; Bochmann, M. *Advanced Inorganic Chemistry*, 6th ed.; Wiley: New York, 1999.
- (2) Palmer, D. A.; van Eldik, R. *Chem. Rev.* **1983**, *83*, 651.
- (3) Culter, A. R.; Hanna, P. K.; Vites, J. C. *Chem. Rev.* **1988**, *88*, 1363.
- (4) Jessop, P. G.; Ikariya, T.; Noyori, R. *Chem. Rev.* **1995**, *95*, 259.
- (5) Gibson, D. H. *Chem. Rev.* **1996**, *96*, 2063.
- (6) Gibson, D. H. *Coord. Chem. Rev.* **1999**, *185–186*, 335.
- (7) Solymosi, F. *J. Mol. Catal.* **1991**, *65*, 337.
- (8) Creutz, C. In *Electrochemical and Electrocatalytic Reactions of Carbon Dioxide*; Sullivan, B. P., Krist, K., Guard, H. E., Eds.; Elsevier: Amsterdam, 1993.
- (9) Kafafi, Z. H.; Hauge, R. H.; Billups, W. E.; Margrave, J. L. *J. Am. Chem. Soc.* **1983**, *105*, 3886 (Li + CO₂).
- (10) Kafafi, Z. H.; Hauge, R. H.; Billups, W. E.; Margrave, J. L. *Inorg. Chem.* **1984**, *23*, 177 (Cs + CO₂).
- (11) Andrews, L.; Tague, T. J., Jr. *J. Am. Chem. Soc.* **1998**, *120*, 13230 (Be + CO₂).
- (12) Solov'ev, V. N.; Polikarpov, E. V.; Nemukhin, A. V.; Sergeev, G. B. *J. Phys. Chem. A* **1999**, *103*, 6721 (Mg + CO₂).
- (13) Zhou, M. F.; Andrews, L. *J. Am. Chem. Soc.* **1998**, *120*, 13230 (Sc, Y + CO₂).
- (14) Mascetti, J.; Tranquille, M. *J. Phys. Chem.* **1988**, *92*, 2177; *Coord. Chem. Rev.* **1999**, *190–192*, 557 (Ti, V, Cr, Fe, Co, Ni, Cu + CO₂).
- (15) Chertihin, G. V.; Andrews, L. *J. Am. Chem. Soc.* **1995**, *117*, 1595 (Ti + CO₂).
- (16) Zhou, M. F.; Andrews, L. *J. Phys. Chem. A* **1999**, *103*, 2066 (Ti, V + CO₂).
- (17) Zhang, L.; Wang, X.; Chen, M.; Qin, Q. *Z. Chem. Phys.* **2000**, *254*, 231 (Zr + CO₂).
- (18) Chen, M.; Wang, X.; Zhang, L.; Qin, Q. *Z. J. Phys. Chem. A* **2000**, *104*, 7010 (Nb + CO₂).
- (19) Wang, X.; Chen, M.; Zhang, L.; Qin, Q. *Z. J. Phys. Chem. A* **2000**, *104*, 758 (Ta + CO₂).
- (20) Souter, P. F.; Andrews, L. *Chem. Commun.* **1997**, 777; *J. Am. Chem. Soc.* **1997**, *119*, 7350 (Cr, Mo, W + CO₂).
- (21) Zhou, M. F.; Liang, B.; Andrews, L. *J. Phys. Chem. A* **1999**, *103*, 2013 (Cr–Zn + CO₂).
- (22) Liang, B.; Andrews, L. *J. Phys. Chem. A* **2002**, *106*, 595 (Re + CO₂).
- (23) Liang, B.; Andrews, L. *J. Phys. Chem. A* **2002**, *106*, 4042 (Os, Ru + CO₂).
- (24) Andrews, L.; Zhou, M. F.; Liang, B.; Li, J.; Bursten, B. E. *J. Am. Chem. Soc.* **2000**, *122*, 11440 (U, Th + CO₂).
- (25) Bulkholder, T. R.; Andrews, L.; Bartlett, R. J. *J. Phys. Chem.* **1993**, *97*, 3500 (B + CO₂).
- (26) Quere, A. M. L.; Xu, C.; Manceron, L. *J. Phys. Chem.* **1991**, *95*, 3031 (Al + CO₂).
- (27) Brock, L. R.; Duncan, M. A. *J. Phys. Chem.* **1991**, *95*, 3031 (Al + CO₂).
- (28) Howard, J. A.; McCague, C.; Sutcliffe, R.; Tse, J. S.; Joly, H. A. *J. Chem. Soc., Faraday Trans.* **1995**, *91*, 799 (Al, Ga + CO₂).
- (29) Himmel, H. J.; Downs, A. J.; Greene, T. M. *Chem. Rev.* **2002**, *102*, 4191, and references therein.
- (30) Papai, I.; Mascetti, J.; Fournier, R. *J. Phys. Chem. A* **1997**, *101*, 4465.
- (31) Fan, H. J.; Liu, C. W. *Chem. Phys. Lett.* **1999**, *300*, 351.
- (32) Sodupe, M.; Branchadell, V.; Rosi, M.; Bauschlicher, C. W., Jr. *J. Phys. Chem. A* **1997**, *101*, 7854.
- (33) See, for example: Xu, C.; Manceron, L.; Perchard, J. P. *J. Chem. Soc. Faraday Trans.* **1993**, *89*, 1291. Bondybey, V. E.; Smith, A. M.; Agreiter, J. *Chem. Rev.* **1996**, *96*, 2113. Fedrigo, S.; Haslett, T. L.; Moskovits, M. *J. Am. Chem. Soc.* **1996**, *118*, 5083. Khriachtchev, L.; Pettersson, M.; Runeberg, N.; Lundell, J.; Rasanen, M. *Nature* **2000**, *406*, 874. Himmel, H. J.; Manceron, L.; Downs, A. J.; Pullumbi, P. *J. Am. Chem. Soc.* **2002**, *124*, 4448. Li, J.; Bursten, B. E.; Liang, B.; Andrews, L. *Science* **2002**, *295*, 2242. Andrews, L.; Wang, X. *Science* **2003**, *299*, 2049.
- (34) Zhou, M. F.; Tsumori, N.; Li, Z.; Fan, K.; Andrews, L.; Xu, Q. *J. Am. Chem. Soc.* **2002**, *124*, 12936. Zhou, M. F.; Xu, Q.; Wang, Z.; von Ragué Schleyer, P. *J. Am. Chem. Soc.* **2002**, *124*, 14854. Jiang, L.; Xu, Q. *J. Am. Chem. Soc.* **2005**, *127*, 42. Xu, Q.; Jiang, L.; Tsumori, N. *Angew. Chem., Int. Ed.* **2005**, *44*, 4338. Jiang, L.; Xu, Q. *J. Am. Chem. Soc.* **2005**, *127*, 8906.
- (35) Baker, A. B.; Andrews, L. *J. Phys. Chem. A* **2006**, *110*, 10419.
- (36) Cheng, P.; Koyanagi, G. K.; Bohme, D. K. *J. Phys. Chem. A* **2006**, *110*, 12832.
- (37) Burkholder, T. R.; Andrews, L. *J. Chem. Phys.* **1991**, *95*, 8697.
- (38) Zhou, M. F.; Tsumori, N.; Andrews, L.; Xu, Q. *J. Phys. Chem. A* **2003**, *107*, 2458. Jiang, L.; Xu, Q. *J. Chem. Phys.* **2005**, *122*, 034505.
- (39) Frisch, M. J.; Trucks, G. W.; Schlegel, H. B.; Scuseria, G. E.; Robb, M. A.; Cheeseman, J. R.; Montgomery, J. A., Jr.; Vreven, T.; Kudin, K. N.; Burant, J. C.; Millam, J. M.; Iyengar, S. S.; Tomasi, J.; Barone, V.; Mennucci, B.; Cossi, M.; Scalmani, G.; Rega, N.; Petersson, G. A.; Nakatsuji, H.; Hada, M.; Ehara, M.; Toyota, K.; Fukuda, R.; Hasegawa, J.; Ishida, M.; Nakajima, T.; Honda, Y.; Kitao, O.; Nakai, H.; Klene, M.; Li, X.; Knox, J. E.; Hratchian, H. P.; Cross, J. B.; Adamo, C.; Jaramillo, J.; Gomperts, R.; Stratmann, R. E.; Yazyev, O.; Austin, A. J.; Cammi, R.; Pomelli, C.; Ochterski, J. W.; Ayala, P. Y.; Morokuma, K.; Voth, G. A.; Salvador, P.; Dannenberg, J. J.; Zakrzewski, V. G.; Dapprich, S.; Daniels, A. D.; Strain, M. C.; Farkas, O.; Malick, D. K.; Rabuck, A. D.; Raghavachari, K.; Foresman, J. B.; Ortiz, J. V.; Cui, Q.; Baboul, A. G.; Clifford, S.; Cioslowski, J.; Stefanov, B. B.; Liu, G.; Liashenko, A.; Piskorz, P.; Komaromi, I.; Martin, R. L.; Fox, D. J.; Keith, T.; Al-Laham, M. A.; Peng, C. Y.; Nanayakkara, A.; Challacombe, M.; Gill, P. M. W.; Johnson, B.; Chen, W.; Wong, M. W.; Gonzalez, C.; Pople, J. A. *Gaussian 03*, revision B.04; Gaussian, Inc.: Pittsburgh, PA, 2003.
- (40) Becke, A. D. *Phys. Rev. A* **1988**, *38*, 3098. Perdew, J. P.; Burke, K.; Wang, Y. *Phys. Rev. B* **1996**, *54*, 16533. Lee, C.; Yang, E.; Parr, R. G. *Phys. Rev. B* **1988**, *37*, 785. Becke, A. D. *J. Chem. Phys.* **1993**, *98*, 5648.
- (41) McLean, A. D.; Chandler, G. S. *J. Chem. Phys.* **1980**, *72*, 5639. Krishnan, R.; Binkley, J. S.; Seeger, R.; Pople, J. A. *J. Chem. Phys.* **1980**, *72*, 650. Frisch, M. J.; Pople, J. A.; Binkley, J. S. *J. Chem. Phys.* **1984**, *80*, 3265.

- (42) Stevens, W.; Basch, H.; Krauss, J. *J. Chem. Phys.* **1984**, *81*, 6026.
Stevens, W. J.; Krauss, M.; Basch, H.; Jasien, P. G. *Can. J. Chem.* **1992**, *70*, 612.
Cundari, T. R.; Stevens, W. J. *J. Chem. Phys.* **1993**, *98*, 5555.
- (43) Darling, J. H.; Ogden, J. S. *J. Chem. Soc., Dalton Trans.* **1972**, 2496.
- (44) Andrews, L.; Zhou, M. F.; Chertihin, G. V.; Bauschlicher, C. W., Jr. *J. Phys. Chem. A* **1999**, *103*, 6525 (Y, La + O₂).
- (45) Zhou, M. F.; Andrews, L.; Bauschlicher, C. W., Jr. *Chem. Rev.* **2001**, *101*, 1931.
- (46) Zhou, M. F.; Andrews, L. *J. Am. Chem. Soc.* **2000**, *122*, 1531.

- (47) Zhou, M. F.; Andrews, L. *J. Phys. Chem. A* **1999**, *103*, 5259.
- (48) Andrews, L.; Zhou, M. F.; Gutsev, G. L.; Wang, X. F. *J. Phys. Chem. A* **2003**, *107*, 561.
Andrews, L.; Zhou, M. F.; Gutsev, G. L. *J. Phys. Chem. A* **2003**, *107*, 990.
- (49) Zhou, M. F.; Chertihin, G. V.; Andrews, L. *J. Chem. Phys.* **1998**, *109*, 10893.
- (50) Zhou, M. F.; Andrews, L. *J. Phys. Chem. A* **1999**, *103*, 6956.
- (51) Zhou, M. F.; Andrews, L. *J. Phys. Chem. A* **1999**, *103*, 7773.
- (52) Liang, B. Y.; Zhou, M. F.; Andrews, L. *J. Phys. Chem. A* **2000**, *104*, 3905.